ELSEVIER

Contents lists available at ScienceDirect

### **Optics Communications**

journal homepage: www.elsevier.com/locate/optcom



## Comparative study of optical nonlinearities of CO $_2$ and N $_2$ O via single-shot spatio-temporally-resolved visualization



Dennis Dempsey<sup>a</sup>, Garima C. Nagar<sup>a</sup>, Jack W. Agnes<sup>a</sup>, Yuxuan Zhang<sup>a</sup>, Nicole A. Batista<sup>a</sup>, Tran-Chau Truong<sup>b</sup>, Devi Sapkota<sup>a</sup>, Michael Chini<sup>b,c</sup>, Bonggu Shim<sup>a,\*</sup>

- <sup>a</sup> Department of Physics, Applied Physics, and Astronomy, Binghamton University, Binghamton, 13902, NY, USA
- <sup>b</sup> Department of Physics, University of Central Florida, Orlando, 32816, FL, USA
- <sup>c</sup> CREOL, the College of Optics and Photonics, University of Central Florida, Orlando, 32816, FL, USA

#### ARTICLE INFO

# Keywords: Nonlinear optics Rotational Raman Nonlinear index of refraction Ultrafast visualization Spectral interferometry Spectral broadening

#### ABSTRACT

We investigate the electronic and rotational Raman optical nonlinearities as well as ionization of  $CO_2$ , which is one of the frequently-used molecules in nonlinear optics, using single-shot spatio-temporally-resolved frequency-domain holography (FDH). As a reference, we also perform FDH measurements using  $N_2O$  whose optical nonlinearities have been studied with single-shot methods previously. Our FDH experiments show that  $CO_2$  exhibits overall smaller optical nonlinearities than  $N_2O$  but has a higher ionization threshold. Furthermore, the FDH results on the delayed rotational Raman response of the molecules are supported by spectral broadening experiments in a gas cell. Our study shows that  $CO_2$  is a highly-nonlinear molecule which is comparable to  $N_2O$  due to a combination of high Raman nonlinearities and high ionization threshold.

Single-shot spatio-temporally-resolved methods are useful and robust for measuring optical nonlinearities with femtosecond time resolutions over hundreds of femtoseconds or picosecond time windows. A few examples of such state-of-the-art single-shot methods are frequency domain holography (FDH) [1,2], single-shot supercontinuum spectral interferometry (SSSI) [3], and orthogonal-geometry time-resolved interferometry [4]. In particular, the key to single-shot techniques like FDH and SSSI is to use chirped probe pulses so that different wavelengths in the chirped probe correspond to different time delays between pump and probe. These techniques have been utilized to study laser wakefields [5,6], laser-atomic-cluster interactions [1,2,7,8], cluster/monomer ratios in supersonic gas jets [1,2], plasma dynamics in gases [1,3,9], the nonlinear index of glass [1,3], nonlinear index and Raman responses of atomic and molecular gases including the main constituents of air [10-12], and plasma dynamics in thin flexible glass under a strong laser field [13].

One of the key targets for nonlinear optics and time-resolved measurements are aligned/rotating linear molecules under strong laser fields [14] due to their important applications in nonlinear optics, for instance, high-order harmonic generation (HHG) [15], laser filamentation [16–20], and spectral broadening [21–24]. Although noble gasses have been used frequently in the past for spectral broadening of ultrashort laser pulses via self-phase modulation (SPM) [25–27], linear molecular gases such as  $N_2$  [22,24],  $N_2$ O [22], and  $CO_2$  [21,23] have been used recently to enhance spectral broadening further via a large contribution of the Raman effect to the nonlinear index. Since the

rotational Raman effect is delayed with respect to the aligning pump pulse, pulses with relatively long durations should be used for effective spectral broadening. For instance, Beetar et al. have used an 80-cycle laser pulse to produce supercontinua with more than two octaves in a capillary filled with  $\rm N_2O$  gas and have generated a 1.6-cycle pulse via post compression [22].  $\rm CO_2$  has also widely been used for spectral broadening previously [23,28] as well as for its rotational dynamics and HHG [29–34]. Although the optical nonlinearities of  $\rm N_2O$  have been studied via single-shot methods [10],  $\rm CO_2$  has not been investigated using single-shot methods despite its potential high optical nonlinearities with applications to various fields of high-intensity laser-matter interactions.

In this Letter we use FDH in order to compare the optical nonlinearities of  $\mathrm{CO}_2$  and  $\mathrm{N}_2\mathrm{O}$  including the instantaneous electronic and rotational Raman responses, and ionization. In addition, we conduct spectral broadening experiments in a gas cell and observe (1) more spectral broadening for  $\mathrm{N}_2\mathrm{O}$  compared with  $\mathrm{CO}_2$  at a given intensity and (2) enhanced broadening with relatively long pulses due to delayed rotational Raman effect for both gases. This observation is in good agreement with our FDH measurements. Our study reveals that  $\mathrm{CO}_2$  is a highly-nonlinear molecule which is comparable to  $\mathrm{N}_2\mathrm{O}$  due to a combination of large Raman nonlinearities and high ionization threshold.

In our FDH setup, the pump centered at 808 nm is 75 fs and the reference and probe centered at 404 nm are chirped to 1.5 ps. The

E-mail address: bshim@binghamton.edu (B. Shim).

Corresponding author.

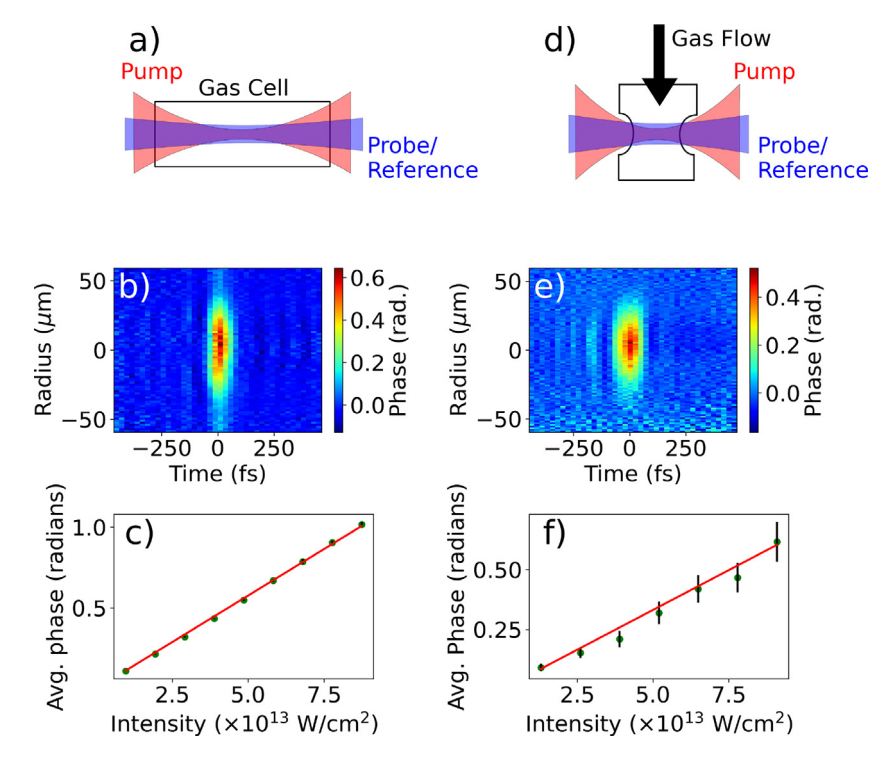


Fig. 1. (a) Experimental setup for FDH using the gas cell. (b) Example of measured spatio-temporal FDH profile of Ar using the gas cell with pump intensity of  $2.1 \times 10^{13}$  W/cm<sup>2</sup>. (c) Linear fit of the measured phase vs. intensity to determine  $n_2$  of Ar. (d) Experimental setup for FDH using the gas jet target. (e) Example of measured spatio-temporal FDH profile of Ar using the gas target with pump intensity of  $9.1 \times 10^{13}$  W/cm<sup>2</sup>. (f) Intensity scan of Ar using the gas target to determine the effective target length ( $L_{ei}$ ) of the gas jet.

reference precedes the pump and the probe measures the nonlinear phase created by the pump-induced optical Kerr effect and plasma. The chirp in the reference/probe enables single-shot measurements by mapping different wavelengths to different time delays. The pump energy is controlled by a combination of a half waveplate and a thin-film polarizer and its polarization is controlled by another half waveplate. Further details of our FDH setup can be found in Ref. [13]. Since gas targets are not susceptible to damage in contrast to solid targets, we use 1-kHz repetition rate and set the exposure time of a spectrometer camera at 25 ms accumulating ~25 laser shots for each data set. We first use a 36-cm long gas cell to confirm the nonlinear index of refraction of Ar  $(\Delta n = n_2 I(r, t))$ , where  $n_2$  is the nonlinear coefficient and I(r, t) is the laser intensity). The pump is focused by a 25-cm focal length lens to an Ar-filled gas cell at 1.3 bar and the focused pump spot size is  $18 \mu m$  $(1/e^2 \text{ radius})$  with a corresponding Rayleigh range  $(z_R)$  of 1.27 mm. The probe/reference spot size is 64  $\mu$ m with corresponding  $z_R$  of 3.2 cm, allowing for complete capture of the pump induced phenomena. We measure the spatio-temporal phase via the optical Kerr effect  $(n_2I)$ in Ar by varying the pump intensity from  $1.3 \times 10^{13}$  to  $9.1 \times 10^{13}$ W/cm<sup>2</sup>. Then we take the average maximum phase from five FDH data sets at each intensity and linearly fit them as a function of intensity using  $\Delta \Phi = 2n_2 I \frac{2\pi}{\lambda} L_{ei}$ , where  $\Delta \Phi$  is the measured phase via cross-phase modulation,  $\lambda$  is the wavelength of the reference pulse, and  $L_{ei} = \pi z_R$ is the effective interaction length for a tightly-focused Gaussian beam in a long gas cell [Fig. 1(b) and (c)]. Using this method we are able to extract  $n_2$  of Ar to be  $9.2 \times 10^{-20}$  cm<sup>2</sup>/W at 1 bar, which is in good agreement with previous studies [17,35-37]. Note that the maximum input peak power used in the experiment (<0.5 GW) is smaller than the critical power for self-focusing for Ar (~7 GW) [38] and thus laser filamentation [39] does not occur.

However, molecules such as  $CO_2$  and  $N_2O$  can induce significant propagation effects in a gas cell due to their highly-nonlinear Raman effect, which can distort the extracted spatio-temporal phase measured by FDH. Thus, to minimize propagation effects, we fabricate a gas jet target with a small interaction length. To fabricate the target we laser

drill two holes with an average hole size of ~200  $\mu m$  in a 1-mm inner diameter glass tube. The cap of the glass tube is blocked by epoxy so that the gas can flow only through the laser-drilled holes. The gas jet target is put in a vacuum chamber and controlled via an x-y-z stage. The target is fed with a backing pressure of 2.7 bar for both gases. In FDH experiments using the gas jet, the focused pump spot size is 21  $\mu m$  (1/e² radius) and the probe/reference spot size is 81  $\mu m$ . In order to determine the effective interaction length for the gas jet, we perform a calibration FDH experiment using Ar by varying the pump intensity [Fig. 1(e) and (f)]. Using the measured  $n_2 = 9.2 \times 10^{-20}$  cm²/W value via FDH with the 36-cm long gas cell and the assumption of a constant gas jet density, we are able to determine the interaction length  $L_{ei}$  of the gas jet to be about 0.8 mm, which is comparable to the inner diameter of the glass tube.

For linear molecules the total nonlinear index of refraction is the sum of the instantaneous electronic contribution  $\Delta n_{elec}(r,t)$  and the rotational Raman contribution which is given by  $\Delta n_{Raman}(r,t)$  $\int_{-\infty}^{t} R(r,t-t')I(r,t')dt'$ , where R(r,t-t') is the rotational Raman response and I(r,t') is the laser intensity profile. The Raman response is due to molecular rotation induced by an aligning pump field and is thus delayed compared with the pump pulse because of their rotational inertia [14]. The electronic ( $\Delta\phi_{elec}$ ) and Raman ( $\Delta\phi_{Raman}$ ) phase contributions can be isolated by separately measuring the phases for parallel pump-probe polarization ( $\Delta\phi_{\parallel}$ ) and orthogonal pump-probe polarization ( $\Delta\phi_{\perp}$ ) (see Fig. 2) and then using the algebraic expressions  $\Delta\phi_{elec} = 3(\Delta\phi_{\parallel} + 2\Delta\phi_{\perp})/5$  and  $\Delta\phi_{Raman} = 2(\Delta\phi_{\parallel} - 3\Delta\phi_{\perp})/5$ . We use this procedure for CO2 and N2O in the gas jet target, extracting the spatio-temporal phase for both the electronic and rotational Raman contributions. We take the average of 30 phase values per intensity from the profiles of the instantaneous and rotational phases, for pump intensities ranging from  $1\times 10^{13}$  to  $6\times 10^{13}$  W/cm<sup>2</sup> for CO<sub>2</sub> and from  $1\times 10^{13}$  to  $4\times 10^{13}$  W/cm<sup>2</sup> for N<sub>2</sub>O. We also take FDH data at higher intensities to study ionization of both gases, which is discussed later. Fig. 3 shows examples of measured instantaneous and delayed Raman responses for CO<sub>2</sub> [Fig. 3(a) and (b)] and N<sub>2</sub>O [Fig. 3(e) and

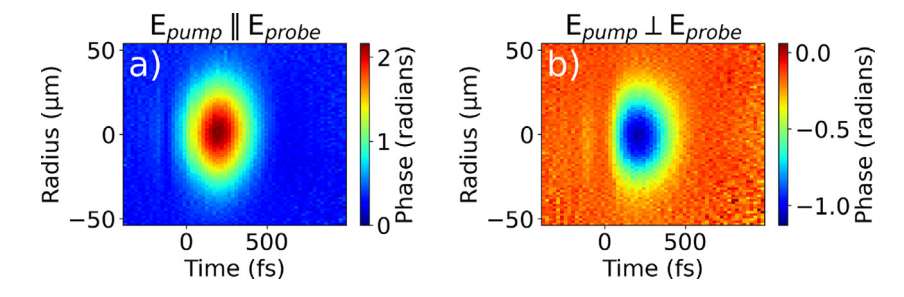


Fig. 2. Examples of FDH data using CO<sub>2</sub> for parallel pump-probe polarization (a) and orthogonal pump-probe polarization (b).

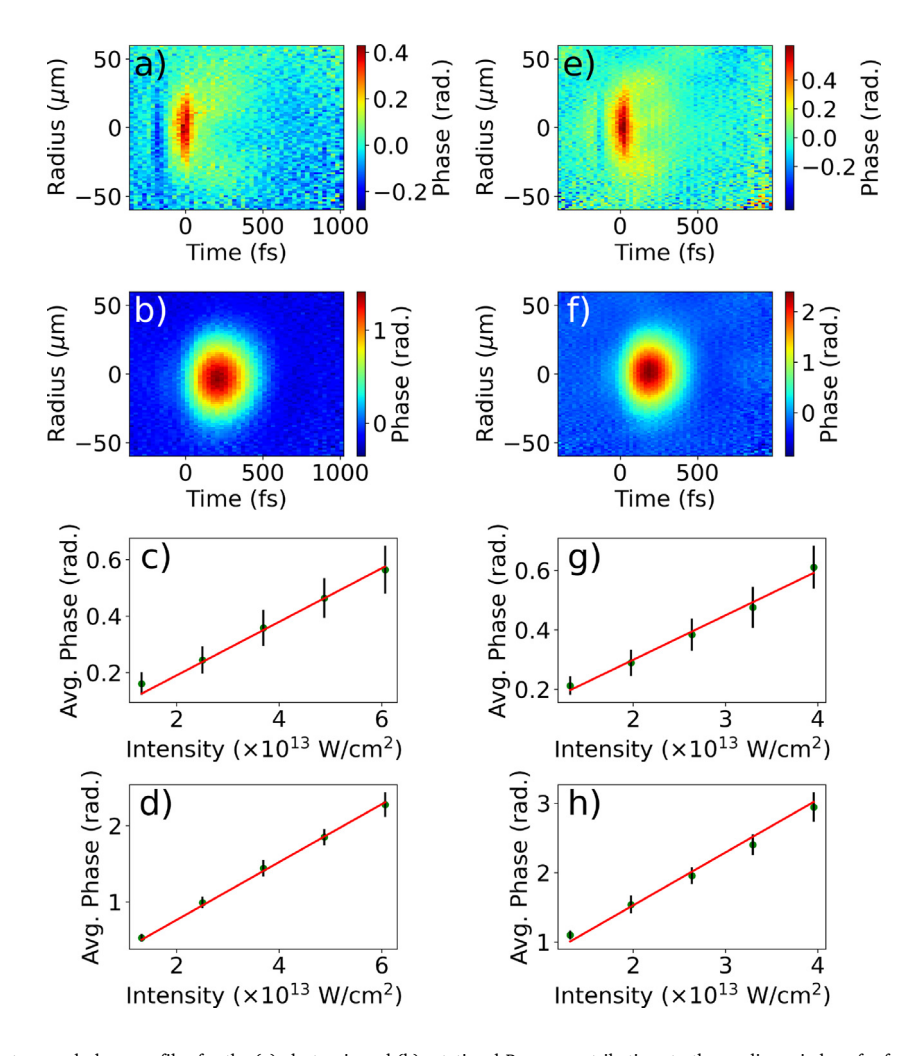


Fig. 3. Examples of the spatio-temporal phase profiles for the (a) electronic and (b) rotational Raman contributions to the nonlinear index of refraction of  $CO_2$  at a pump intensity of  $3.8 \times 10^{13}$  W/cm². Linear fit of the average maximum phase as a function of intensity for the (c) electronic and (d) rotational Raman contributions for  $CO_2$ . Examples of the spatio-temporal phase profiles for the (e) electronic and (f) rotational contribution to the nonlinear index of refraction of  $N_2O$  at a pump intensity of  $4 \times 10^{13}$  W/cm². Linear fit of the maximum phase as a function of intensity for the (g) electronic and (h) rotational Raman contributions for  $N_2O$ .

(f)]. By fitting the average maximum phase as a function of pump intensity for both the instantaneous and delayed Raman responses, we can determine the instantaneous nonlinear coefficient  $n_2$  as well as the anisotropy of the polarizability of the molecule ( $\Delta\alpha$ ). First, we measure  $n_2$  at 1 bar to be  $13 \times 10^{-20}$  cm<sup>2</sup>/W for CO<sub>2</sub> [Fig. 2(c)] and  $21 \times 10^{-20}$  cm<sup>2</sup>/W for N<sub>2</sub>O [Fig. 2(g)].

Next, we extract  $\Delta \alpha$  using perturbative density matrix model calculations for rotational Raman effects of molecules [10] and comparing them to the isolated rotational phases measured via FDH. The

calculated index change due to the Raman effect is given by [10]

$$\Delta n_{Raman} = -\frac{16\pi^2 N (\Delta \alpha)^2}{15\hbar n_0 c} \left[ \sum_j \frac{j(j-1)}{2j-1} \left( \frac{\rho_j}{2j+1} - \frac{\rho_{j-2}}{2j-3} \right) \right] \times Im \left( e^{i\omega t} \int_{-\infty}^t I(t') e^{-i\omega t'} dt' \right), \tag{1}$$

where *N* is the gas number density,  $\hbar$  is the reduced Plank's constant,  $n_0$  is the linear refractive index, c is the speed of light, I(t') is the laser intensity,  $\omega = 4\pi c B(2j-1)$  is the Raman angular frequency

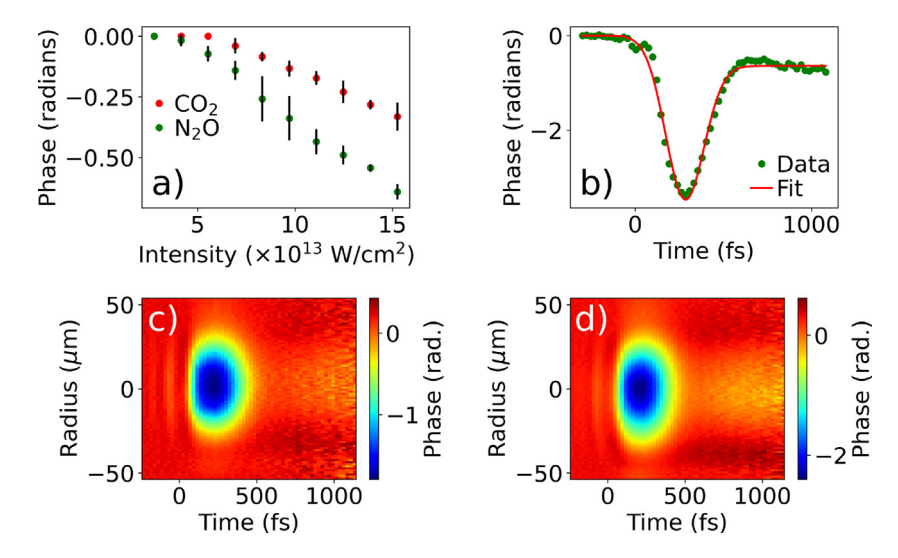


Fig. 4. (a) Result of fitting on-axis (r = 0) phase lineouts to extract the phase change due to plasma as a function of pump intensity. We start to see ionization effects near  $7 \times 10^{13}$  W/cm<sup>2</sup> for CO<sub>2</sub> and  $5 \times 10^{13}$  W/cm<sup>2</sup> for N<sub>2</sub>O. (b) Example of on-axis lineout with fit. (c) and (d) Examples of FDH data showing plasma effects at pump intensity of  $1.1 \times 10^{14}$  W/cm<sup>2</sup> [(c) CO<sub>2</sub> and (d) N<sub>2</sub>O.].

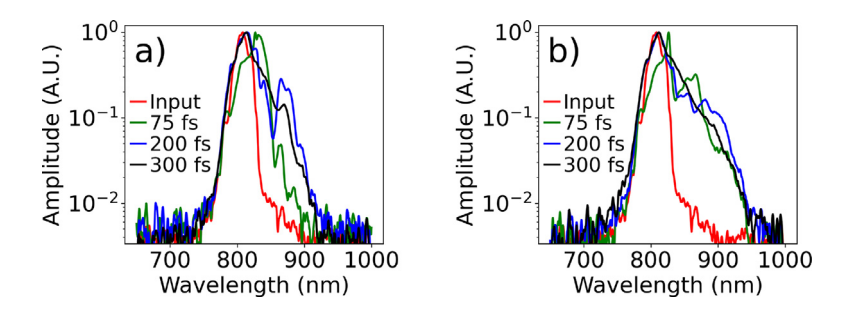


Fig. 5. Spectral broadening in a long gas cell filled with 2-bars of (a)  $CO_2$  and (b)  $N_2O$  using 808-nm laser pulses at 75, 200, and 300 fs pulse durations. We observe more spectral broadening with pulses whose durations are  $\geq$ 200 fs, which is in good agreement with the delayed Raman peaks of  $CO_2$  and  $N_2O$  shown in Fig. 2 (b) and (f).

of the molecule, B is the rotational constant (0.41 cm<sup>-1</sup> for N<sub>2</sub>O and 0.3902 cm<sup>-1</sup> for CO<sub>2</sub> [40]), and  $\rho_j$  is the density matrix for the unperturbed molecular system given by

$$\rho_{j} = \frac{D_{j}(2j+1)e^{\frac{-hcBj(j+1)}{k_{B}T}}}{\sum_{i} D_{i}(2i+1)e^{\frac{-hcBi(j+1)}{k_{B}T}}},$$
(2)

where  $D_j$  is the statistical weighting factor (1 for both N<sub>2</sub>O and CO<sub>2</sub>),  $k_B$  is Boltzmann's constant, and T is the ambient temperature. Here we can ignore the damping/dephasing factor due to its long time scale (tens of ps). Using linear fitting (see Fig. 2(d) for CO<sub>2</sub> and Fig. 2(h) for N<sub>2</sub>O), we measure  $\Delta\alpha$  to be 22.7 × 10<sup>-25</sup> cm³ and 16.3 × 10<sup>-25</sup> cm³ for N<sub>2</sub>O and CO<sub>2</sub>, respectively. The measured  $\Delta\alpha$  for N<sub>2</sub>O is in very good agreement with previous work (~28 × 10<sup>-25</sup> cm³) [35,40].

We also investigate ionization of  $CO_2$  and  $N_2O$  via FDH using higher pump intensities. We use perpendicular polarization between pump and probe/reference because it is much easier to visualize the plasma-induced negative phase with perpendicular polarization than with the parallel case. After taking FDH data, we fit the on-axis (r=0) phase using the function:  $C_1e^{-2(t-t')^2/t_p^2} + C_2(1+erf\left[C_3(t-t')\right])/2$ , where  $C_1$ ,  $C_2$ ,  $C_3$ ,  $t_p$  and t' are the fitting parameters and erf represents the error function [41]. Here the first Gaussian term accounts for the phase due to the electronic and rotational Raman contributions and the second term accounts for the phase due to plasma with a long recombination time (~ps). Then we extract the average plasma-induced phase  $C_2$  from 8 different spatio-temporal profiles and plot as a function of pump intensity to compare ionization between  $CO_2$  and  $N_2O$  (Fig. 4). We start

to see ionization effects near  $7\times10^{13}~W/cm^2$  for  $CO_2$  and  $5\times10^{13}~W/cm^2$  for  $N_2O$ . The higher ionization threshold for  $CO_2$  is in good agreement with the fact that the ionization energy of  $CO_2$  is higher (13.78 eV) than that of  $N_2O$  (12.89 eV). Since determination of the ionization threshold depends on measurement sensitivity, we think that the actual ionization thresholds may be smaller than those measured by FDH

Lastly, to corroborate the FDH experiments, we conduct measurements of spectral broadening in a gas cell by varying the pulse duration at a fixed nominal intensity. We use a 1-meter long gas cell filled with CO<sub>2</sub> or N<sub>2</sub>O at 2 bar, and we focus the 808-nm pulse using a 75-cm focal length lens with a spot size of 95 µm near the center of the gas cell. We then vary the pulse duration using the laser pulse compressor. To keep the same nominal intensity of  $2 \times 10^{13}$  W/cm<sup>2</sup>, we adjust the laser pulse energy using a thin-film polarizer and a half waveplate. For spectrum measurements, we put a diffusive plate near the output window of the gas cell and record the spectrum reflected off it using a fiber spectrometer. As shown in Fig. 5, we observe more spectral broadening for N2O compared with CO2 at a given intensity due to the larger Raman effect of N2O as measured by FDH. In addition, we see enhanced broadening with relatively long pulses (≥200 fs), which corresponds well to the delayed Raman peaks of CO2 and N2O as shown in Fig. 3. Although N2O exhibits more spectral broadening than CO2 at a given intensity, spectral broadening with CO2 can be further enhanced due to its higher ionization threshold. Since the nonlinear index contribution from the rotational Raman effect is much larger than that from the electronic effect (see Fig. 3), the Raman effect mainly contributes to the spectral broadening. In particular, spectral red shifts are dominant because the Stokes Raman process should be the main contributor due to more population in the ground state at room temperature [22]. Moreover, since the shortest (75 fs) pulse duration in our experiment is long enough to be affected by the dominant Raman response and the peak intensity is small for the instantaneous electronic response, we observe minimal spectral blue shifts caused by SPM.

In conclusion, we compare the nonlinear optical properties of  $\rm CO_2$  and  $\rm N_2O$  including the instantaneous and rotational Raman contributions to the nonlinear index of refraction and ionization thresholds, as well as spectral broadening. Our FDH measurements show that  $\rm N_2O$  is more nonlinear than  $\rm CO_2$  but we find that the ionization threshold of  $\rm CO_2$  is higher than that of  $\rm N_2O$ , potentially allowing for using higher intensities in experiments without ionization. These results should contribute to a fundamental understanding of high-intensity laser-matter interactions using linear molecules such as  $\rm CO_2$ , which is one of the frequently-used molecules in various fields of nonlinear optics. Furthermore, single-shot FDH can potentially be used for measuring molecular vibrations if the pump pulse is very short [42,43]. In addition, it can be used for other molecular gases such as  $\rm N_2$ ,  $\rm O_2$ , and  $\rm H_2$  [10] and also liquids and solids as long as the measured phase is not excessive.

#### Declaration of competing interest

The authors declare that they have no known competing financial interests or personal relationships that could have appeared to influence the work reported in this paper.

#### Data availability

Data will be made available on request

#### **Funding**

U.S. Air Force Office of Scientific Research (AFOSR) (FA9550-18-1-0223 and FA9550-20-1-0284), National Science Foundation (NSF), USA (PHY-2010365), DOE Basic Energy Sciences, USA (DE-SC0019291), IEEC of Binghamton University, USA.

#### References

- [1] S.P. Le Blanc, E.W. Gaul, N.H. Matlis, A. Rundquist, M.C. Downer, Single-shot measurement of temporal phase shifts by frequency-domain holography, Opt. Lett. 25 (10) (2000) 764–766.
- [2] X. Gao, A.V. Arefiev, R.C. Korzekwa, X. Wang, B. Shim, M.C. Downer, Spatio-temporal profiling of cluster mass fraction in a pulsed supersonic gas jet by frequency-domain holography, J. Appl. Phys. 114 (3) (2013) 034903.
- [3] K.Y. Kim, I. Alexeev, H.M. Milchberg, Single-shot supercontinuum spectral interferometry, Appl. Phys. Lett. 81 (22) (2002) 4124–4126.
- [4] G.C. Nagar, D. Dempsey, B. Shim, Wavelength scaling of electron collision time in plasma for strong field laser-matter interactions in solids, Commun. Phys. 4 (1) (2021) 96.
- [5] N.H. Matlis, S. Reed, S.S. Bulanov, V. Chvykov, G. Kalintchenko, T. Matsuoka, P. Rousseau, V. Yanovsky, A. Maksimchuk, S. Kalmykov, G. Shvets, M.C. Downer, Snapshots of laser wakefields, Nat. Phys. 2 (11) (2006) 749–753.
- [6] P. Dong, S.A. Reed, S.A. Yi, S. Kalmykov, Z.Y. Li, G. Shvets, N.H. Matlis, C. McGuffey, S.S. Bulanov, V. Chvykov, G. Kalintchenko, K. Krushelnick, A. Maksimchuk, T. Matsuoka, A.G.R. Thomas, V. Yanovsky, M.C. Downer, Holographic visualization of laser wakefields. New J. Phys. 12 (4) (2011) 045016.
- [7] K.Y. Kim, I. Alexeev, E. Parra, H.M. Milchberg, Time-resolved explosion of intense-laser-heated clusters, Phys. Rev. Lett. 90 (2003) 023401.
- [8] I. Alexeev, T.M. Antonsen, K.Y. Kim, H.M. Milchberg, Self-focusing of intense laser pulses in a clustered gas, Phys. Rev. Lett. 90 (2003) 103402.
- [9] J.K. Wahlstrand, Y.-H. Cheng, Y.-H. Chen, H.M. Milchberg, Optical nonlinearity in Ar and N<sub>2</sub> near the ionization threshold, Phys. Rev. Lett. 107 (2011) 103901.
- [10] Y.-H. Chen, S. Varma, A. York, H.M. Milchberg, Single-shot, space- and time-resolved measurement of rotational wavepacket revivals in  $H_2$ ,  $D_2$ ,  $N_2$ ,  $O_2$ , and  $N_2O$ , Opt. Express 15 (18) (2007) 11341–11357.

- [11] S. Zahedpour, J.K. Wahlstrand, H.M. Milchberg, Measurement of the nonlinear refractive index of air constituents at mid-infrared wavelengths, Opt. Lett. 40 (24) (2015) 5794–5797.
- [12] S. Zahedpour, S.W. Hancock, H.M. Milchberg, Ultrashort infrared 2.5-11 μm pulses: spatiotemporal profiles and absolute nonlinear response of air constituents, Opt. Lett. 44 (4) (2019) 843–846.
- [13] D. Dempsey, G.C. Nagar, C.K. Renskers, R.I. Grynko, J.S. Sutherland, B. Shim, Single-shot ultrafast visualization and measurement of laser-matter interactions in flexible glass using frequency domain holography, Opt. Lett. 45 (5) (2020) 1252–1255.
- [14] H. Stapelfeldt, T. Seideman, Colloquium: Aligning molecules with strong laser pulses, Rev. Modern Phys. 75 (2003) 543–557.
- [15] R. Velotta, N. Hay, M.B. Mason, M. Castillejo, J.P. Marangos, High-order harmonic generation in aligned molecules, Phys. Rev. Lett. 87 (2001) 183901.
- [16] J.R. Peñano, P. Sprangle, P. Serafim, B. Hafizi, A. Ting, Stimulated Raman scattering of intense laser pulses in air, Phys. Rev. E 68 (2003) 056502.
- [17] E.T.J. Nibbering, G. Grillon, M.A. Franco, B.S. Prade, A. Mysyrowicz, Determination of the inertial contribution to the nonlinear refractive index of air, N<sub>2</sub>, and O<sub>2</sub> by use of unfocused high-intensity femtosecond laser pulses, J. Opt. Soc. Amer. B 14 (3) (1997) 650–660.
- [18] S. Varma, Y.-H. Chen, H.M. Milchberg, Trapping and destruction of long-range high-intensity optical filaments by molecular quantum wakes in air, Phys. Rev. Lett. 101 (2008) 205001.
- [19] F. Calegari, C. Vozzi, S. Gasilov, E. Benedetti, G. Sansone, M. Nisoli, S. De Silvestri, S. Stagira, Rotational Raman effects in the wake of optical filamentation, Phys. Rev. Lett. 100 (2008) 123006.
- [20] N. Berti, P. Béjot, J.-P. Wolf, O. Faucher, Molecular alignment and filamentation: Comparison between weak- and strong-field models, Phys. Rev. A 90 (2014) 053851.
- [21] R.A. Bartels, T.C. Weinacht, N. Wagner, M. Baertschy, C.H. Greene, M.M. Murnane, H.C. Kapteyn, Phase modulation of ultrashort light pulses using molecular rotational wave packets, Phys. Rev. Lett. 88 (2001) 013903.
- [22] J.E. Beetar, M. Nrisimhamurty, T.-C. Truong, G.C. Nagar, Y. Liu, J. Nesper, O. Suarez, F. Rivas, Y. Wu, B. Shim, M. Chini, Multioctave supercontinuum generation and frequency conversion based on rotational nonlinearity, Sci. Adv. 6 (34) (2020) eabb5375.
- [23] V.N. Bagratashvili, V.M. Gordienko, E.I. Mareev, N.V. Minaev, A.V. Ragulskaya, F.V. Potemkin, Supercontinuum generation under filamentation driven by intense femtosecond pulses in supercritical xenon and carbon dioxide, Russ. J. Phys. Chem. B 10 (8) (2016) 1211–1215.
- [24] P.A. Carpeggiani, G. Coccia, G. Fan, E. Kaksis, A. Pugžlys, A. Baltuška, R. Piccoli, Y.-G. Jeong, A. Rovere, R. Morandotti, L. Razzari, B.E. Schmidt, A.A. Voronin, A.M. Zheltikov, Extreme Raman red shift: ultrafast multimode nonlinear spacetime dynamics, pulse compression, and broadly tunable frequency conversion, Optica 7 (10) (2020) 1349–1354.
- [25] Y.-G. Jeong, R. Piccoli, D. Ferachou, V. Cardin, M. Chini, S. Hädrich, J. Limpert, R. Morandotti, F. Légaré, B.E. Schmidt, L. Razzari, Direct compression of 170-fs 50-cycle pulses down to 1.5 cycles with 70% transmission, Sci. Rep. 8 (1) (2018) 11794.
- [26] J.E. Beetar, F. Rivas, S. Gholam-Mirzaei, Y. Liu, M. Chini, Hollow-core fiber compression of a commercial Yb:KGW laser amplifier, J. Opt. Soc. Amer. B 36 (2) (2019) A33–A37.
- [27] G.C. Nagar, B. Shim, Study of wavelength-dependent pulse self-compression for high intensity pulse propagation in gas-filled capillaries, Opt. Express 29 (17) (2021) 27416–27433.
- [28] J. Wu, H. Cai, Y. Peng, H. Zeng, Controllable supercontinuum generation by the quantum wake of molecular alignment, Phys. Rev. A 79 (2009) 041404.
- [29] C. Vozzi, F. Calegari, E. Benedetti, J.-P. Caumes, G. Sansone, S. Stagira, M. Nisoli, R. Torres, E. Heesel, N. Kajumba, J.P. Marangos, C. Altucci, R. Velotta, Controlling two-center interference in molecular high harmonic generation, Phys. Rev. Lett. 95 (2005) 153902.
- [30] K. Miyazaki, M. Kaku, G. Miyaji, A. Abdurrouf, F.H.M. Faisal, Field-free alignment of molecules observed with high-order harmonic generation, Phys. Rev. Lett. 95 (2005) 243903.
- [31] T. Kanai, S. Minemoto, H. Sakai, Quantum interference during high-order harmonic generation from aligned molecules, Nature 435 (7041) (2005) 470–474.
- [32] X. Zhou, R. Lock, W. Li, N. Wagner, M.M. Murnane, H.C. Kapteyn, Molecular recollision interferometry in high harmonic generation, Phys. Rev. Lett. 100 (2008) 073902.
- [33] H.J. Wörner, J.B. Bertrand, P. Hockett, P.B. Corkum, D.M. Villeneuve, Controlling the interference of multiple molecular orbitals in high-harmonic generation, Phys. Rev. Lett. 104 (2010) 233904.
- [34] L. He, S. Sun, P. Lan, Y. He, B. Wang, P. Wang, X. Zhu, L. Li, W. Cao, P. Lu, C.D. Lin, Filming movies of attosecond charge migration in single molecules with high harmonic spectroscopy, Nature Commun. 13 (1) (2022) 4595.
- [35] J.K. Wahlstrand, Y.-H. Cheng, H.M. Milchberg, Absolute measurement of the transient optical nonlinearity in N<sub>2</sub>, O<sub>2</sub>, N<sub>2</sub>O, and Ar, Phys. Rev. A 85 (2012) 043820.

- [36] V. Loriot, E. Hertz, O. Faucher, B. Lavorel, Measurement of high order Kerr refractive index of major air components, Opt. Express 17 (16) (2009) 13429-13434
- [37] D.P. Shelton, J.E. Rice, Measurements and calculations of the hyperpolarizabilities of atoms and small molecules in the gas phase, Chem. Rev. 94 (1) (1994)
- [38] G. Fibich, A.L. Gaeta, Critical power for self-focusing in bulk media and in hollow waveguides, Opt. Lett. 25 (2000) 335.
- [39] A. Couairon, A. Mysyrowicz, Femtosecond filamentation in transparent media, Phys. Rep. 441 (2007) 47.
- [40] C.H. Lin, J.P. Heritage, T.K. Gustafson, R.Y. Chiao, J.P. McTague, Birefringence arising from the reorientation of the polarizability anisotropy of molecules in collisionless gases, Phys. Rev. A 13 (1976) 813–829.
- [41] J.K. Wahlstrand, S. Zahedpour, A. Bahl, M. Kolesik, H.M. Milchberg, Boundelectron nonlinearity beyond the ionization threshold, Phys. Rev. Lett. 120 (2018) 183901.
- [42] A.M. Zheltikov, Raman response function of atmospheric air, Opt. Lett. 32 (14) (2007) 2052–2054.
- [43] J. Odhner, R. Levis, Optical spectroscopy using gas-phase femtosecond laser filamentation, Annu. Rev. Phys. Chem. 65 (1) (2014) 605–628.